

Comparative Oxidative Addition of Transition-Metal Iodocyclopentadienyl Complexes ($\eta^5\text{-C}_5\text{H}_4\text{-I}$) ML_n ($\text{M} = \text{Re}, \text{Mn}, \text{Fe}$) with a Palladium(0) Complex: Relevance to the Efficiency of Catalytic Reactions

Christian Amatore,[†] Béatrice Godin,[†] Anny Jutand,^{*,†} Benoit Ferber,[‡] Siden Top,[‡] and Gérard Jaouen[‡]

Département de Chimie, Ecole Normale Supérieure, CNRS, 24 Rue Lhomond, 75231 Paris Cedex 5, France, and Ecole Nationale Supérieure de Chimie de Paris, CNRS, 11 Rue Pierre et Marie Curie, 75231 Paris Cedex 5, France

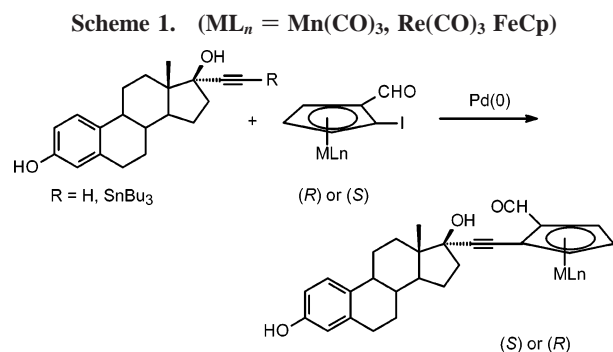
Received March 28, 2007

Summary: The rate constants of the oxidative addition of the transition-metal iodocyclopentadienyl complexes ($\eta^5\text{-C}_5\text{H}_4\text{-I}$) ML_n ($\text{ML}_n = \text{Mn}(\text{CO})_3$ (**1a**), $\text{Re}(\text{CO})_3$ (**1b**), CpFe (**1c**)) with $\text{Pd}^0(\text{PPh}_3)_4$ have been determined in DMF. As expected, the oxidative addition is faster for the electron-acceptor groups $\text{Mn}(\text{CO})_3$ and $\text{Re}(\text{CO})_3$ than for the electron-donor group FeCp , with the reactivity order **1a** > **1b** > **1c**. Comparison of the rate constants of the oxidative additions affords a new strategy for the evaluation of the electronic properties of transition-metal units ligated to the iodocyclopentadienyl moiety with the following decreasing electron-acceptor properties: $\text{Mn}(\text{CO})_3 > \text{Re}(\text{CO})_3 > \text{FeCp}$. The complexes formed in the oxidative addition are characterized as *trans*- $[(\eta^5\text{-C}_5\text{H}_4)\text{PdI}(\text{PPh}_3)_2]\text{ML}_n$ ($\text{ML}_n = \text{Mn}(\text{CO})_3$ (**2a**), $\text{Re}(\text{CO})_3$ (**2b**), CpFe (**2c**)) with the decreasing stability order in DMF: **2c** > **2b** > **2a**. The relevance to the efficiency of palladium-catalyzed Stille or Sonogashira reactions from related complexes **1** is discussed.

Introduction

In a study of the molecular recognition of planar chiralities by the α form of the estrogen receptor, the formyl-substituted transition-metal iodocyclopentadienyl complexes (*R*)- and (*S*)- $[\eta^5\text{-C}_5\text{H}_3\text{-1-I-2-(CHO)]ML}_n$ ($\text{ML}_n = \text{Mn}(\text{CO})_3$, $\text{Re}(\text{CO})_3$, CpFe) have been engaged in palladium-catalyzed reactions with alkynyl derivatives of estradiol: Stille reactions ($\text{R} = \text{SnBu}_3$) and Sonogashira reactions ($\text{R} = \text{H}$) (Scheme 1).¹

The ferrocenyl products ($\text{ML}_n = \text{CpFe}$) were mainly obtained in a Sonogashira reaction, whereas the cyrhetrenyl ($\text{ML}_n = \text{Re}(\text{CO})_3$) and cymantrenyl ($\text{ML}_n = \text{Mn}(\text{CO})_3$) products were mainly formed in a Stille reaction.¹ All reactions involve a common first step: the oxidative addition of (*R*)- or (*S*)- $[\eta^5\text{-C}_5\text{H}_3\text{-1-I-2-(CHO)]ML}_n$ with a $\text{Pd}(0)$ complex. In a first approach, the difference in reactivity seems to depend on the type of reaction, Stille versus Sonogashira: i.e., on the nucleophilic attack (transmetalation) on σ -cyclopentadienyl– $\text{Pd}(\text{II})$ complexes formed in the oxidative addition of the iodocyclopentadienyl derivatives. However, the effective rates of the successive steps in a catalytic cycle are not independent from each other. Indeed, catalytic reactions are more efficient if the rates of the different steps of the catalytic cycle are made as



close as possible to each other.² For example, a catalytic reaction may be not efficient, because the oxidative addition is too fast in comparison to the rate of the transmetalation which follows this first step. This may even be amplified whenever the products formed after the fast oxidative addition are not stable. Indeed, the overall catalytic reaction would not work, because a transmetalation that is too slow will allow a significant degradation of the accumulating intermediate. It is thus worthwhile to investigate the rate and mechanism of the oxidative addition first.

We wish therefore to report here kinetic data on the reactivity of the related iodocyclopentadienyl complexes ($\eta^5\text{-C}_5\text{H}_4\text{-I}$) ML_n ($\text{ML}_n = \text{Mn}(\text{CO})_3$ (**1a**), $\text{Re}(\text{CO})_3$ (**1b**), CpFe (**1c**); Chart 1) in their oxidative addition with $\text{Pd}^0(\text{PPh}_3)_4$ in DMF.

Results and Discussion

Kinetics of the Oxidative Addition. The reactivity of **1a** with $\text{Pd}^0(\text{PPh}_3)_4$ ($C_0 = 2.2 \text{ mM}$) in DMF containing $n\text{Bu}_4\text{NBF}_4$ (0.3 M) was followed by means of electrochemical techniques,^{3,4} on the basis of the fact that the oxidation current of $\text{Pd}^0(\text{PPh}_3)_3$ (the major complex generated from $\text{Pd}^0(\text{PPh}_3)_4$) must decrease after addition of **1a**, due to a decay of its concentration in the oxidative addition (eq 1 in Scheme 2). This analytical technique can be used only if the $\text{Pd}(0)$ complex is more easily oxidized than the reagents involved in the oxidative addition. The electrochemical properties of complexes **1a–c** were first investigated to compare their oxidation potentials with that of $\text{Pd}^0(\text{PPh}_3)_3$. The oxidation peaks of **1a–c** were all located at

* To whom correspondence should be addressed. Tel: 33144323872. Fax: 33144323325. E-mail: Anny.Jutand@ens.fr.

[†] Ecole Normale Supérieure.

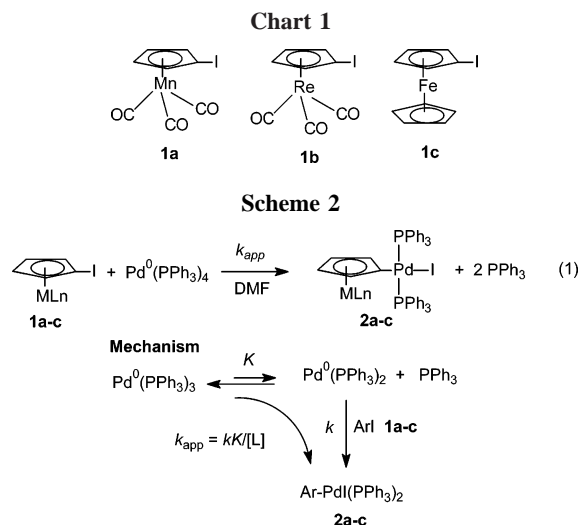
[‡] Ecole Nationale Supérieure de Chimie de Paris.

(1) Ferber, B.; Top, S.; Vessières, A.; Welter, R.; Jaouen, G. *Organometallics* 2006, 25, 5730–5739.

(2) Amatore, C.; Jutand, A. *J. Organomet. Chem.* 1999, 576, 254–278.

(3) Fauvarque, J. F.; Pflüger, F.; Troupel, M. *J. Organomet. Chem.* 1981, 208, 419–427.

(4) Amatore, C.; Jutand, A.; Khalil, F.; M'Barki, M. M.; Mottier, L. *Organometallics* 1993, 12, 3168–3178.



potentials more positive than that of $\text{Pd}^0(\text{PPh}_3)_3$ ($E^{\text{P}} = +0.083$ V vs SCE (irrev)): $E^{\text{P}}_{\mathbf{1a}} = +0.47$ V (irrev), $E^{\text{P}}_{\mathbf{1b}} = +0.55$ V (irrev), $E^{\text{P}}_{\mathbf{1c}} = +0.72$ V (rev). Consequently, the kinetics of the oxidative addition of **1a** with $\text{Pd}^0(\text{PPh}_3)_3$ could be monitored by recording the decay versus time of the oxidation current of $\text{Pd}^0(\text{PPh}_3)_3$ at a rotating-gold-disk electrode polarized at +0.1 V.

The oxidative addition was performed in the presence of $n = 1, 5,$ and 10 equiv of **1a**. The use of correct kinetic laws was required, taking into account the variation of the concentration of the phosphine released in the course of the oxidative addition (see mechanism in Scheme 2). x is the molar fraction of the $\text{Pd}(0)$ at t : $x = [\text{Pd}(0)_t]/[\text{Pd}(0)_0] = i^{\text{ox}}_t/i^{\text{ox}}_0$.

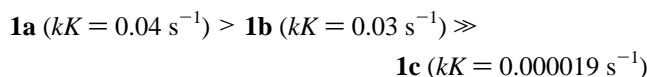
$$n = 1: X_1 = 2 - \ln x - 2/x = -kKt \quad (\text{a})$$

$$n = 5: X_5 = \{\ln x - 3 \ln[(4+x)/5]\}/2 = -kKt \quad (\text{b})$$

$$n = 10: X_{10} = (2 \ln x - x + 1)/10 = -kKt \quad (\text{c})$$

Within this formulation, plotting X_n ($n = 1, 5, 10$) against time gave the same straight line irrespective of n , thus attesting to first-order reactions for both **1a** and $\text{Pd}^0(\text{PPh}_3)_4$ (Figure 1a). The value of kK , which characterizes the reactivity of **1a**, was determined from the slope of the common regression line. The same reactions were performed with **1b** (Figure 1b) and **1c** (Figure 1c). The reactivity order is displayed in Chart 2. Just for comparison, let us recall that the oxidative addition of iodobenzene, performed under the same conditions at 20°C , is characterized by $kK = 0.05 \text{ s}^{-1}$.⁴

Chart 2 (DMF, 25°C)



Complex **1a** is slightly more reactive than complex **1b**, and both are considerably more reactive than complex **1c** (Chart 2). The oxidative addition of aryl halides with $\text{Pd}^0(\text{PPh}_3)_4$ is faster when the aryl group is substituted by an electron-acceptor group⁵ (Hammett correlation with a positive slope).³ The kinetic results established here are in full agreement with this rule, since $\text{Mn}(\text{CO})_3$ and $\text{Re}(\text{CO})_3$ are electron-acceptor groups, whereas the $\text{Fe}(\text{Cp})$ group is an electron-donor group. Comparison of the rate constants of the oxidative addition allows an easy

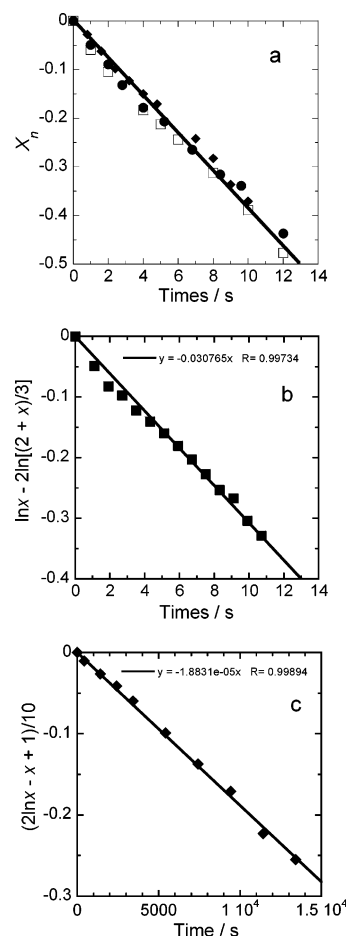


Figure 1. Kinetics of the oxidative addition of $\text{Pd}^0(\text{PPh}_3)_4$ ($C_0 = 2.2$ mM) in DMF at 25°C . (a) For **1a**, plot of X_n (see text) versus time: $n = 1$ (\square), 5 (\bullet), 10 equiv (\blacklozenge) of **1a**. (b) For **1b** (3 equiv), plot of $X_3 = \ln x - 2 \ln[(2+x)/3]$ versus time. (c) For **1c** (10 equiv), plot of X_{10} (see text) versus time.

classification of the electronic properties of ML_n groups as electron-acceptor groups onto a cyclopentadienyl ring (Chart 3).

Chart 3. Decreasing Electron-Acceptor Properties of ML_n



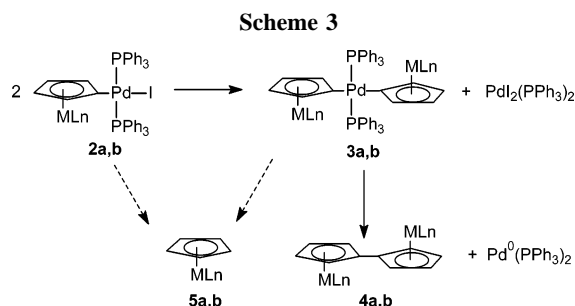
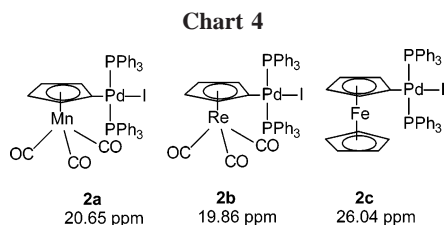
Pd(II) Complexes Formed in the Oxidative Addition. The complexes $\text{trans}[(\eta^5\text{-C}_5\text{H}_4)\text{PdI}(\text{PPh}_3)_2]\text{ML}_n$ (**2a-c**), generated in the oxidative addition, were characterized by ^1H and ^{31}P NMR spectroscopy. All complexes exhibited a ^{31}P NMR singlet indicative of a trans coordination of the two PPh_3 ligands on the Pd(II) center (Chart 4). One related complex has been reported by Basset et al. in the oxidative addition of $\text{Pd}^0(\text{PPh}_3)_4$ with a phenyl chloride whose phenyl group was η^6 -coordinated to the electron-acceptor group $\text{Cr}(\text{CO})_3$.⁶

Complexes **2a,b** were not as stable and underwent ligand scrambling at long reaction times, according to the reactions reported in Scheme 3.

The reactions were followed by ^{31}P and ^1H NMR, focusing on the protons of the cyclopentadienyl moieties. To an NMR tube containing $\text{Pd}^0(\text{PPh}_3)_4$ in acetone- d_6 was added a stoichiometric amount of **1a**. The first ^1H NMR recorded after 8 min displayed the signals of **2a** (5.64 (d, $J = 2$ Hz, 2H) and 5.74

(5) Fitton, P.; Rick, E. A. *J. Organomet. Chem.* **1971**, *28*, 287–288.

(6) Dufaud, V.; Thivole-Cazat, J.; Basset, J. M.; Mathieu, R.; Jaud, J.; Waissermann, J. *Organometallics* **1991**, *10*, 4005–4015.

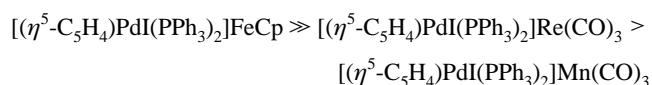


ppm ($d, J = 2$ Hz, 2H)) and those of unreacted **1a**. After 35 min, the signals of **1a** were no longer detected, attesting to the completion of the oxidative addition. The complex $\text{CpMn}(\text{CO})_3$ (**5a**; δ 4.8 ppm (s)) was observed, as well as a new intermediate complex at 4.35 (br s, 2H) and 4.49 ppm (br s, 2H), associated with a ^{31}P NMR singlet at 22.72 ppm. The latter disappeared with time as well as **2a**, leading to $\text{PdI}_2(\text{PPh}_3)_2$, $\text{CpMn}(\text{CO})_3$ (**5a**), and the dimer complex **4a** (δ 5.94 (br s, 2H) and 6.06 ppm (br s, 2H)). $\text{PdI}_2(\text{PPh}_3)_2$ was isolated as red crystals and characterized by an X-ray structure analysis and a ^{31}P NMR singlet at δ 12.93 ppm. After 4 h 15 min, the ^1H NMR spectrum only exhibited the signals of $\text{CpMn}(\text{CO})_3$ (**5a**) and the dimer complex **4a**. The signals of the intermediate complex were assigned to complex **3a**. Ligand scrambling from **2a** gave **3a**, which must undergo reductive elimination, leading to the dimeric complex **4a** and $\text{Pd}^0(\text{PPh}_3)_2$ (Scheme 3). Complex **5a** may be formed from **2a** or **3a** by a reaction with protons or by H^+ abstraction (Scheme 3). The scrambling reaction was also observed when investigating the kinetics of the reaction of **1a** with $\text{Pd}^0(\text{PPh}_3)_4$ under the condition of a relatively slow oxidative addition: i.e., $n = 1$ equiv of **1a**. One indeed notices that the oxidation current at a rotating-gold-disk electrode of the $\text{Pd}(0)$ complex (proportional to its concentration) did not drop to zero but decreased and then increased to a fixed value equal to 80% of the initial value. Upon further addition of 1 equiv of **1a**, the oxidation current dropped again and then increased. The oxidation current dropped to zero upon addition of iodobenzene (10 equiv), establishing that the species which appeared while the oxidative addition proceeded was a $\text{Pd}(0)$ complex or a species in equilibrium with the initial reactive $\text{Pd}(0)$ complex and that this $\text{Pd}(0)$ complex was regenerated through spontaneous evolution of **2a** ($2a \rightarrow 3a \rightarrow 4a$ in Scheme 3). The scrambling reaction was thus followed by cyclic voltammetry performed at a stationary-gold-disk electrode. The oxidation peak of $\text{Pd}^0(\text{PPh}_3)_3$ (2.2 mM in DMF) at $E^p = +0.083$ V vs SCE disappeared upon addition of **1a** (1 equiv), but a new oxidation peak appeared at less positive potential at +0.029 V. It disappeared upon addition of PhI . Consequently, the new oxidation peak characterized $\text{Pd}^0(\text{PPh}_3)_3$, whose oxidation peak had been shifted because the concentration of the free PPh_3 had varied upon oxidative addition (see mechanism in Scheme 2) due to the formation of $\text{PdI}_2(\text{PPh}_3)_2$. Furthermore, the reduction peak of $\text{PdI}_2(\text{PPh}_3)_2$ at $E^p_{\text{red}} = -0.95$ V was observed when the cyclic voltammetry was performed first toward reduction potentials, giving support to the formulation in Scheme 3.

A similar scrambling reaction was also observed from complex **2b**, after addition of a stoichiometric amount of **1b** to $\text{Pd}^0(\text{PPh}_3)_4$ in an NMR tube containing acetone- d_6 . The first ^1H NMR recorded after 24 min displayed the signals of **2b** at 6.18 ($d, J = 2$ Hz, 2H) and 6.07 ppm ($d, J = 2$ Hz, 2H), along with those of unreacted **1b**. After 67 min, the signals of **1b** were no longer detected, attesting to the completion of the oxidative addition. In addition to the signals of complex **2b**, the singlet of the complex $\text{CpRe}(\text{CO})_3$ (**5b**; δ 5.49 ppm (s)) was observed as well as the signals of the dimer complex **4b** (δ 5.94 (br s, 2H) and 6.05 ppm (br s, 2H)). $\text{PdI}_2(\text{PPh}_3)_2$ was also detected on the ^{31}P NMR spectrum. Complex **2b** gave complex **4b** with time. After 4 h, the ^1H NMR spectrum exhibited the singlet of **5b** and the two sets of signals of complexes **2b** and **4b** (ratio 1:1). The signals of the intermediate complex **3b** were hardly detected due to low stationary concentration.

Upon comparing the evolution of complexes **2a,b** with time, one concludes that **2a** is less stable than **2b**. No scrambling reaction was observed from complex **2c** generated in the slowest oxidative addition (Chart 5).

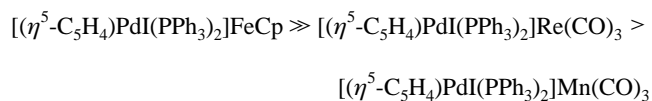
Chart 5. Decreasing Stability Order of Complexes **2a–c**



Therefore, the stability order of complexes **2a–c** is opposite to the reactivity order of **1a–c** in their oxidative addition. The slowest oxidative addition gave the most stable complex and vice versa.

In conclusion, the complexation of the iodocyclopentadienyl ligand by transition-metal complexes in $(\eta^5\text{-C}_5\text{H}_4\text{-I})\text{ML}_n$ ($\text{ML}_n = \text{Mn}(\text{CO})_3, \text{Re}(\text{CO})_3, \text{CpFe}$) affects the rate of its oxidative addition with $\text{Pd}^0(\text{PPh}_3)_4$ in DMF. As expected, iodocyclopentadienyl moieties ligated to the electron-acceptor groups ($\text{Mn}(\text{CO})_3, \text{Re}(\text{CO})_3$) give a faster oxidative addition than these moieties ligated to an electron-donor group (FeCp) (Chart 2). Therefore, investigation of the rate of the oxidative addition of a $\text{Pd}(0)$ complex affords a new strategy which allows the classification of the electronic properties of transition-metal groups as ligands of the iodocyclopentadienyl moiety⁷ with the decreasing electron-acceptor properties: $\text{Mn}(\text{CO})_3 > \text{Re}(\text{CO})_3 \gg \text{FeCp}$.

The most stable complex, *trans*- $[(\eta^5\text{-C}_5\text{H}_4)\text{PdI}(\text{PPh}_3)_2]\text{FeCp}$, is the one which is formed in the slowest oxidative addition with the decreasing stability order



In palladium-catalyzed reactions, once the complexes *trans*- $[(\eta^5\text{-C}_5\text{H}_4)\text{PdI}(\text{PPh}_3)_2]\text{ML}_n$ (**2**) are generated in the oxidative addition, their decomposition competes with their reaction with the nucleophiles of Stille or Sonogashira reactions (transmeta-

(7) Since their structures strongly differ, their electronic properties cannot be compared by IR spectroscopy, which is restricted to CO vibrations. The ^1H NMR shifts of the protons of the Cp-I group in the complexes **1a–c** could be compared and used to estimate the electronic properties of $\text{Mn}(\text{CO})_3, \text{Re}(\text{CO})_3$, and FeCp . In CDCl_3 the chemical shifts are 4.67 and 5.00 ppm for complex **1a**,⁸ 4.70 and 5.00 ppm for complex **1b**,⁸ and 4.15 and 4.41 ppm for **1c**.⁹ From these data, we conclude that the FeCp group is less electron accepting than $\text{Mn}(\text{CO})_3$ and $\text{Re}(\text{CO})_3$, but the latter two cannot be distinguished and classified. A comparison of the rate constants of the oxidative addition provides a better classification for the three organometallic moieties (see text).

lation steps). Catalytic reactions are more efficient if the rates of the different steps of the catalytic cycle are made as close as possible to each other.² One can thus predict that (i) slow transmetalation steps will favor the efficiency of catalytic reactions involving $(\eta^5\text{-C}_5\text{H}_4\text{-I})\text{FeCp}$ (slowest oxidative addition) and (ii) fast transmetalation steps will favor the efficiency of catalytic reactions of $(\eta^5\text{-C}_5\text{H}_4\text{-I})\text{Mn}(\text{CO})_3$ or $(\eta^5\text{-C}_5\text{H}_4\text{-I})\text{Re}(\text{CO})_3$ involved in fast oxidative additions, bypassing decomposition of the Pd(II) complexes formed in the oxidative addition. The high stability of complex **2c** (FeCp) formed in the slowest oxidative addition must be more compatible with the slow nucleophilic attack of $\text{RC}\equiv\text{CCu}$ (present at catalytic concentration) in Sonogashira reactions. This is why the Sonogashira reaction appeared to be more efficient with the coordinated FeCp reagent in Scheme 1.¹ The faster nucleophilic attack of $\text{RC}\equiv\text{C-SnBu}_3$ (present at stoichiometric concentration) in Stille reactions is more adapted to the fast oxidative additions of complexes **1a,b**. Moreover, the complexation of the active Pd(0) complex by the $\text{C}\equiv\text{C}$ bond of $\text{RC}\equiv\text{C-SnBu}_3$ should occur, as established for $\text{CH}_2=\text{CH-SnBu}_3$ and $\text{RC}\equiv\text{CH}$ derivatives.¹⁰ This complexation would slow down the oxidative addition of **1a,b** and thus favor the efficiency of the catalytic Stille reaction by bringing the rate of the oxidative addition closer to that of the transmetalation step. This affords an educated explanation of the fact that the Stille reactions were found to be more efficient with the coordinated $\text{Mn}(\text{CO})_3$ and $\text{Re}(\text{CO})_3$ reagents than with the coordinated Fe(Cp) (Scheme 1).¹

Experimental Section

General Considerations. ³¹P NMR spectra were recorded on a Bruker spectrometer (101 MHz) with H_3PO_4 as an external reference. ¹H NMR spectra were recorded on a Bruker spectrometer (250 MHz, TMS). Cyclic voltammetry and amperometry were performed at gold-disk electrodes with a homemade potentiostat and a Tacussel GSTP4 waveform generator. The voltammograms were recorded on a Nicolet 301 oscilloscope. All experiments were performed under an argon atmosphere.

Chemicals. DMF was distilled from calcium hydride under vacuum and kept under argon. The complexes **1a**,⁸ **1b**,⁸ **1c**,⁹ and $\text{Pd}^0(\text{PPh}_3)_4$ ¹¹ were synthesized as detailed in the literature.

General Procedure for the Kinetics of the Oxidative Addition of $(\eta^5\text{-C}_5\text{H}_4\text{-I})\text{ML}_n$ (1a-c**) with $\text{Pd}^0(\text{PPh}_3)_4$.** Experiments were

carried out in a three-electrode thermostated cell (25 °C) connected to a Schlenk line. The reference was a saturated calomel electrode (Radiometer) separated from the solution by a bridge filled with 3 mL of DMF containing $n\text{Bu}_4\text{NBF}_4$ (0.3 M). The counter electrode was a platinum wire of ca. 1 cm² apparent surface area. A 13.5 mL portion of DMF containing $n\text{Bu}_4\text{NBF}_4$ (0.3 M) was introduced into the cell followed by 34.7 mg (0.03 mmol) of $\text{Pd}^0(\text{PPh}_3)_4$. Cyclic voltammetry was performed at a stationary-gold-disk electrode (diameter 2 mm) at a scan rate of 0.2 V s⁻¹. The kinetic measurements for the oxidative addition of **1a** were performed at a rotating-gold-disk electrode (Radiometer, EDI 65109, diameter 2 mm, angular velocity 105 rad s⁻¹) polarized at +0.1 V vs SCE. A 99 mg portion (0.3 mmol) of **1a** dissolved in 0.2 mL of DMF was added, and the decrease of the oxidation current of $\text{Pd}^0(\text{PPh}_3)_3$ was recorded versus time until total conversion. Cyclic voltammetry and ³¹P NMR spectroscopy were performed just afterward.

Characterization of $[(\eta^5\text{-C}_5\text{H}_4)\text{PdI}(\text{PPh}_3)_2]\text{Mn}(\text{CO})_3$ (2a**).** To 5.6 mg (4.8 μmol) of $\text{Pd}^0(\text{PPh}_3)_4$ in 500 μL of acetone-*d*₆ was added 4.4 mg (13.5 μmol) of **1a**. After 30 min, the acetone solution was poured into 100 mL of diethyl ether. A red precipitate of **2a** was formed, contaminated by some $\text{CpMn}(\text{CO})_3$, which was separated and isolated as light yellow crystals by dissolution of the crude precipitate into chloroform. Its ¹H NMR in CDCl_3 was similar to that of an authentic sample (see text). The red solid **2a** was isolated and characterized. ¹H NMR (250 MHz, acetone-*d*₆, TMS): δ 5.64 (d, *J* = 2 Hz, 2H), 5.74 (d, *J* = 2 Hz, 2H), 7.22 (m, 4H), 7.38 (m, 2H), 7.49 (m, 4H), 7.79 (m, 4H), 7.93 (m, 8H), 7.98 (m, 4H), 8.05 ppm (m, 4H). ¹³C NMR (62.9 MHz, acetone-*d*₆, TMS): δ 206.16 ppm (CO), instead of 225 ppm in **1a**. ³¹P NMR (101 MHz, acetone-*d*₆): δ 20.65 ppm (s).

Characterization of $[(\eta^5\text{-C}_5\text{H}_4)\text{PdI}(\text{PPh}_3)_2]\text{Re}(\text{CO})_3$ (2b**).** To 7.5 mg (6.8 μmol) of $\text{Pd}^0(\text{PPh}_3)_4$ in 500 μL of acetone-*d*₆ was added 8.9 mg (19.4 μmol) of **1b**. After 30 min, the acetone solution was poured into 100 mL of diethyl ether. A red precipitate of **2b** was formed. ¹H NMR (250 MHz, acetone-*d*₆): δ 6.18 (d, *J* = 2 Hz, 2H), 6.07 (d, *J* = 2 Hz, 2H), 7.35 (m, 4H), 7.51 (m, 6H), 7.83 (m, 12H), 8.12 ppm (m, 8H). ³¹P NMR (101 MHz, acetone-*d*₆): δ 19.86 ppm (s).

Characterization of $[(\eta^5\text{-C}_5\text{H}_4)\text{PdI}(\text{PPh}_3)_2]\text{FeCp}$ (2c**).** To 6 mg (5.2 μmol) of $\text{Pd}^0(\text{PPh}_3)_4$ in 500 μL of acetone-*d*₆ was added 3 mg (9.3 μmol) of **1c**. After 12 h, the acetone solution was poured into 100 mL of diethyl ether. A brown precipitate of **2c** was isolated and characterized. ¹H NMR (250 MHz, acetone-*d*₆): δ 4.16 (s, 5H), 4.67 (d, *J* = 2 Hz, 2H), 4.92 (d, *J* = 2 Hz, 2H), 7.42 (m, 12H), 7.65 (m, 6H), 7.72 ppm (m, 12H). ³¹P NMR (101 MHz, acetone-*d*₆): δ 26.04 ppm (s).

Acknowledgment. This work has been supported in part by the Centre National de la Recherche Scientifique (UMR CNRS-ENS-UPMC 8640, UMR-CNRS 7576), the Ministère de la Recherche (Ecole Normale Supérieure and Ecole Nationale Supérieure de Chimie de Paris), and ANR FerVect (ANR-06-blanc-0387-01). We thank Johnson Matthey for a loan of palladium salt.

OM700302U

(8) Lynch, T. J.; Diminguez, R.; Helvenston, M. C. *Organometallics* **1988**, *7*, 2566–2567.

(9) Guillauneux, D.; Kagan, H. B. *J. Org. Chem.* **1995**, *60*, 2502–2505.

(10) (a) For the complexation of Pd(0) by alkynes, see: Amatore, C.; Bensalem, S.; Ghalem, S.; Jutand, A.; Medjour, Y. *Eur. J. Org. Chem.* **2004**, 366–371. (b) For the complexation of Pd(0) by vinylstannanes, see: Amatore, C.; Bucaille, A.; Fuxa, A.; Jutand, A.; Meyer, M.; Ndedi Ntepe, A. *Chem. Eur. J.* **2001**, *7*, 2134–2142. (c) For a review see: Jutand, A. *Pure Appl. Chem.* **2004**, *76*, 565–576.

(11) Rosevear, D. T.; Stone, F. G. A. *J. Chem. Soc. A* **1968**, 164–167.